

Depth Discrimination with 2D Haptics During Static Viewing of 3D Angiograms

Dingrong Yi and Vincent Hayward

Haptics Laboratory, Center for Intelligent Machines
McGill University, Montréal, Canada

Abstract. We describe a force feedback scheme that is able to provide for haptic depth perception for use during the static 2D viewing of 3D angiograms. The scheme returns 2D horizontal forces that bear some analogy with forces that would be needed to glide a virtual proxy on the vessel centerlines. The display system was evaluated by asking subjects to determine the relative depth of randomly selected points on vessel segments. The results indicate that subjects were able to discriminate the relative depth in an average time of 12 seconds and with an accuracy of 95%.

1 Introduction

The judgement of relative depth is a commonly needed skill when visualizing three-dimensional data sets. Regardless of the domain, almost all methods devoted to conveying depth artificially rely on computer graphics and take advantage of various depth cues including transparency, shading, intensity, color, rotation, perspective, and so on, sometimes combined with symbolic markers made of numbers, words, or special symbols.

Here, we investigate a 2D haptic cue designed to convey depth which is applicable to data in the form of space curves and which can be produced by inexpensive devices. Such space curves are encountered, for example, with 3D angiograms. Usability was assessed by eliminating all graphic depth cues and testing subjects' ability to discriminate depth based on this haptic cue alone.

Depth perception when viewing graphic displays has been an active subject of study and many methods exist for volumetric data visualization [14] [17] [4] [12] [3] [8]. In most of these cases the underlying data set is acquired in 3D (e.g. X-ray

computed Tomography (CT) and Magnetic Resonance Imaging (MRI)) and one problem is to convey depth in the display. A commonly used technique is the maximum intensity projection method (MIP), whereby voxels are projected on a two dimensional plane using a principle which, in fact, recalls how X-ray images are produced (See Fig. 3, background). But unlike an X-ray image which represents the accumulated opacity along a ray, a MIP displays only the voxels with maximal intensity along the rays.

Angiograms are such that their shape can be represented by a tree of space curves that can be extracted from the raw data by skeletonization. The resulting object appears on a screen as a set of intertwined lines, Fig. 1a. This display is economical in graphic space usage, but conveys no depth information. Asked to decide the depth relationship between two points of this skeleton, a viewer without knowledge of the cerebral anatomy would perform at chance. A shaded surface rendering of the vessel system, see Fig. 1b, provides thickness and some indication of orientation, but is more cluttered.

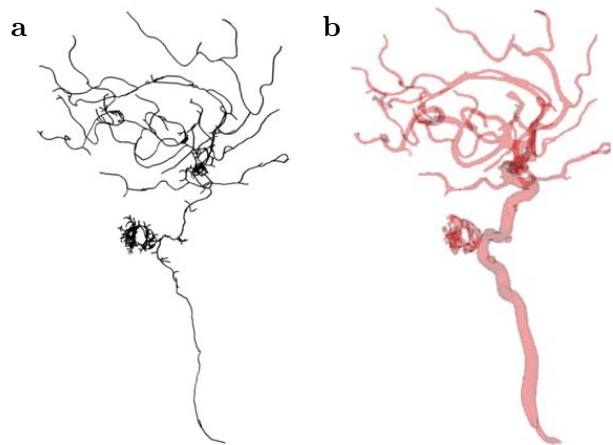


Fig. 1. **a)** Projection of the skeleton of a cerebral angiogram. **b)** Same skeleton represented as a tubular object with shading.

D. Yi is now with the Dept. of Automation and Computer-Aided Engineering, Chinese University of Hong Kong.

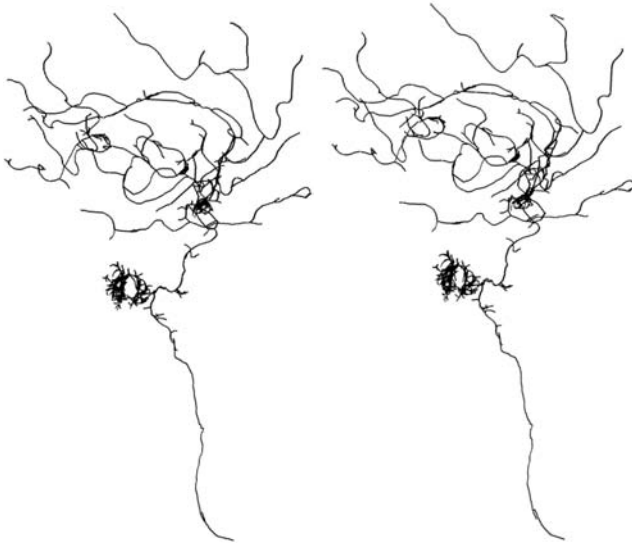


Fig. 2. Stereoscopic pair. It may be fused into a 3D image by uncrossing the eyes so that the left eye sees the left panel and the right eye sees the right panel. It is possible to realize that, despite the apparent complexity of the projection, the vessel system is actually divided into two subsystems, one in the back and one in the front.

Fig. 2 shows a stereo pair to demonstrate the three-dimensional nature of the data. Fig. 3 represents the same data but with depth coded as color and overlaid on the maximum intensity projection of the complete data set to create a context closer to actual practice. It is now evident that much of the depth information is exploitable, however the availability of color to represent some other important aspect of the data, such as blood flow, is now lost.

In general, the visualization problem of angiograms is a challenging one because angiograms are visualized in conjunction with other images to provide additional anatomical and functional information about the same patient. A powerful approach to convey depth graphically is to rotate the 3D data set to create motion cues in the 2D image [17]. While it is possible to rotate complex MIP displays at interactive rates [7], [5], [13], this approach also has limitations. For example, if a MIP display is used in conjunction with another modalities (such as CT) which cannot be rotated, then they cannot be overlaid. Stereopsis is similarly limited in its ability to provide for the simultaneous viewing of several combined data sets.

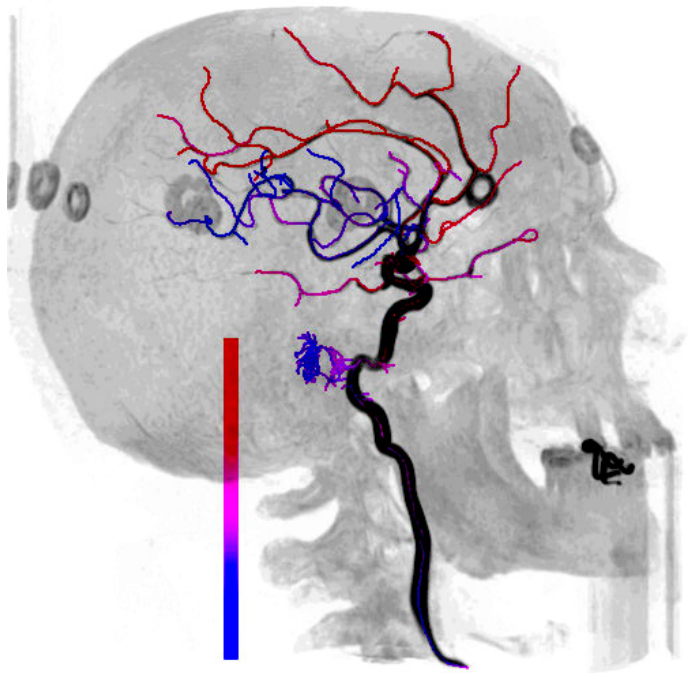


Fig. 3. Skeleton registered with a maximum intensity projection display (MIP) with depth coded by color (red: close, blue: far).

Using actual images obtained from computed rotational angiography, we investigate whether or not untrained users succeeded in using minimal 2D haptics to discriminate the relative depth of sections of a static angiogram presented graphically. Our main objective was to provide a technique which could be combined with any other depth presentation techniques and could be added to the toolbox of interface designers.

2 Related Work

Avila and Sobierajski developed a graphic-haptic visualization system to display and modify volume data sets [2]. Shi and Pai reconstructed a 3D shape based on a stereo image pair, and presented it using a force based on the gradient of depth in an effort to help the user detect contour changes [16]. Pao and Lawrence have proposed a collection of haptic representation modes for rendering scalar fields in the 3D domain [15]. A viscosity scalar field was mapped to a damping impedance, pseudo-gravity was mapped to an attractive force, topography was rendered by the height of a virtual surface. Infed *et al.* implemented a graphic-haptic rendering system

to address the visualization problem in magnetic fields, fluid dynamic, and stress analysis with a 5 DOF haptic interface [10]. The visual display of the magnetic streamline direction was a vector tangent to it, and the corresponding haptic feedback was a torque that forced the stylus to maintain alignment with the streamline to convey whether it was oriented toward or away from the viewer.

With the exception of target acquisition as in GUI interaction tasks, not much attention has been given to the quantitative evaluation of the effectiveness of haptic feedback, especially when graphic and haptic representations map the data set in an integrated manner, hence, there is not much work that could provide a basis for comparison. Iwata and Noma reported that position error was reduced by a factor of two as compared to visual modality alone when either or both of force and torque were enabled [11]. In their 3D display system, the force was based on density gradient, torque about z on density. Their visual stimuli was provided through a head-mounted display and the haptic device was a 6 DOF master manipulator.

In the case of curve tracing tasks, there were some controversial reports on the usefulness of haptic feedback. Hurmuzlu et al. reported that force feedback did not significantly affect the subjects' performance in tracing curves and that it neither reduced the task completion time nor improved the tracing accuracy [9]. Wang found instead that haptic force feedback was helpful during 2D boundary tracing by reducing the task completion time [18].

3 Usability Study

Usability is generally understood to be the degree of the efficiency and satisfaction with which users can achieve tasks. We sought to demonstrate that it was possible to gain the perception of depth using a plain 2D static visual display augmented with 2D haptic feedback. The experiment was aimed at showing that with force feedback, most subjects had an excellent level of depth discrimination while viewing angiograms, but when the force feedback was removed, their performance reverted to essentially chance level.

Whereas the centerline of vessels could be superposed onto the MIP display to enhance contrast, in order to eliminate depth information resulting from the background anatomy, the visual display

used in the experiment provided the vessel skeleton only. The graphic display did not provide depth cues such as intensity, color, shading, or others. It was only used to locate the vessels on the screen. The display provided all the depth cues haptically, in the form of forces that depended on the movements of the user and on the shape of the vessels.

3.1 Task

The task was to discriminate the depth relationship between two randomly designated locations on cerebral vessels, of which only a projection was viewed. The locations were indicated on the screen by two visible dots overlaid on the graphic display. One was green and the other red. The subjects were asked to make a decision about which of the two points was closer to the viewer. The actual distance between these two dots ranged 15 mm to 52 mm in length. The depth was either monotonically increasing or decreasing from the red to the green dot. However, the subjects were not informed of this fact before the experiment. Given that the purpose of this study was to show feasibility independently from human perceptual capabilities, these conditions were selected to yield a force feedback stimulus that was most of the time clearly above threshold. Segments with very small depth changes were not eliminated and subjects were free to adjust the force feedback gain if they felt that it was difficult to make a decision.

3.2 Display

The system consisted of a personal computer, a haptic device, and a color video monitor configured to operate at 1200 x 1024 pixel resolution. The study was carried out with the PenCat/Pro™ haptic device briefly described here.



Fig. 4. Haptic device.

The device, see Fig. 4, had three-degree-of-freedom of input movement but only two-degree-

of-freedom of force output in the horizontal plane. The protruding arm held a spherically jointed stylus and was passively actuated in the vertical direction so as to return naturally to a neutral position 2.0 cm from the table surface. It could deflect vertically by ± 0.8 cm from this neutral position. The rectangular workspace size was 14.0×10.0 cm. The device was programmed to return forces that did not exceed 4.0 N. Since it was direct-driven, when the force feedback was turned off, it could move freely with no perceivable friction and inertia.

3.3 Operating Modes

There were two operating modes associated with the vertical input: a re-indexing mode and a force reflecting mode.

The re-indexing mode was needed because force feedback haptic devices have a fixed absolute working space. This makes it difficult to adjust the relationship between hand movement and cursor movement. Re-indexing is a common solution to this problem and was implemented here. When lifting the stylus, cursor was decoupled from the user input (just like an ordinary mouse) and no force feedback was provided.

When working in the force reflecting mode, the force intensity was dependent on the vertical deflection. There was first a dead zone, then a proportional intensity zone, and a saturation zone. This was useful because when the device was left unattended there was no force feedback.

In addition, when desired the subject could turn the force feedback off simply by releasing the grip. It also created a smooth transition that prevented any sudden and distracting force jump. In the saturation zone, the force intensity was entirely determined by the computer. The size of these zones were 2, 8, and 5 mm. The overall intensity could be adjusted via a slider bar for optimal comfort (≤ 4.0 N).

3.4 Visual Display

The visual display consisted of a complicated network of 3D piecewise smooth and continuous curves extracted from an actual angiogram. Those curves mingled, overlapped, connected, and branched off. This represented the centerlines of the cerebral vessels extracted from a true 3D volumetric CRT angiogram [19]. To prevent a subject

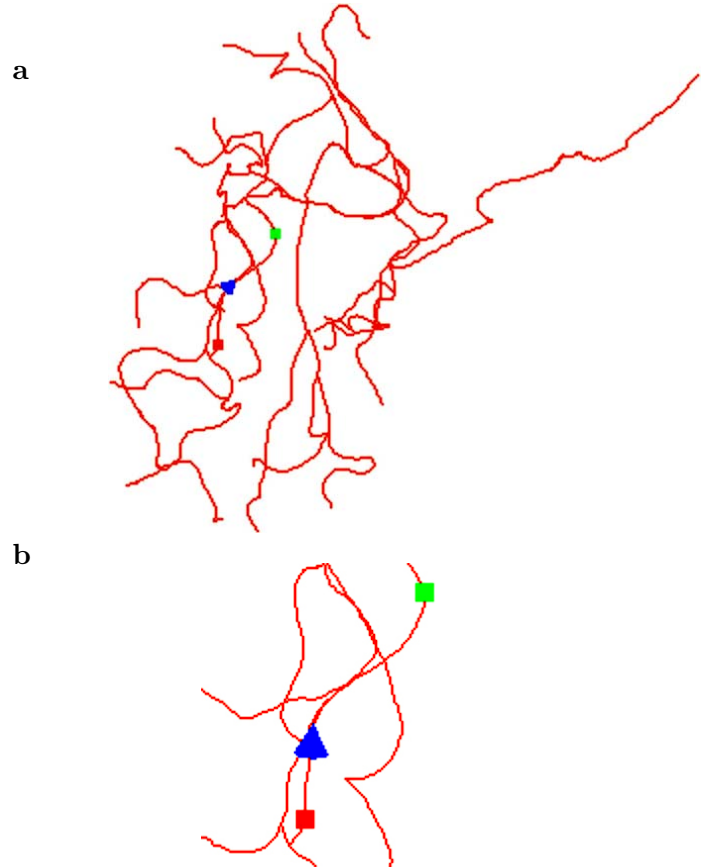


Fig. 5. **a.** Example of visual display. **b** Enlargement.

from guessing its structure, the MIP display of the angiogram was turned off. The lines were rendered in red on a white background into a 500 pixels by 500 pixels square window.

The appearance depended on the perspective projection on the screen. During the experimental trials, the network of space curves was fixed but the viewing direction and the clipping window was changed randomly.

The two colored dots gave no information of depth (see Fig. 5 for one example). A cursor of the shape of a cone drawn in solid blue was used to visually indicate the interaction point at all times. It was programmed to assist the user to trace the vessels. It oriented itself automatically along the local tangent of the vessel centerline, pointing towards the moving direction. It was rendered at a fixed depth. The update rate of the visual stimulus was 40 times per second.

3.5 Haptic Feedback

The haptic feedback was specifically designed to indicate depth changes. The two-dimensional force feedback was designed to produce an analogy with a virtual object sliding like a bead in a gravity field along a frictionless space curve. However, the analogy was only superficial as explained next. The force was computed as a product of three factors, each supplying a different piece of information.

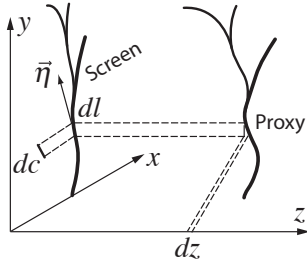


Fig. 6. The vessel network was projected along z for viewing. The virtual proxy moved in 3D, so that to a seen displacement dl corresponded a depth change dz of the proxy.

Fig. 6 represents a network of space curves projected on a screen in x - y coordinates. When the subject moved the haptic interface by distance dh (not shown), this movement mapped to the movement dc of an invisible point c on the screen. The cursor visible on the screen moved by dl obtained by projecting dc onto the tangent of the visible curve. The visible cursor was thus automatically guided to move along the local tangent $\vec{\eta}$, even with approximate user input. In “virtual space” this corresponds to the movement of a virtual interaction point — the bead — sliding on the centerline and changing depth. The force returned was:

$$\vec{F} = -k \frac{dz}{dl} \vec{\eta} \quad (1)$$

This scheme can be described as follows:

1. The factor k was simply an intensity factor. It was such that when the handle was in the vicinity of its rest position, its value was zero. When depressing the handle further toward the table, it increased until a maximum yielding a comfortable level of force feedback. In this manner the force intensity did not depend on how much the handle was depressed, yet the force feedback was easily turned on or off as desired by the subject.

2. The second factor was designed to inform the user of the change of depth of the interaction point, precisely the information which was lost in the viewing projection. It was the ratio of the change of depth dz over the corresponding distance dl covered by the user. The analogy with gravity does not hold since moving orthogonally to a centerline would produce no force.

3. The third factor $\vec{\eta}$, a unit vector, informed the user of the direction of the projected bead movement and therefore supplemented information gained visually. Thus, the direction of rendered forces was along $\vec{\eta}$ (Fig. 6). But of course, the *actual* force returned to the user was horizontal.

One effect of the varying direction force was to help the subject move along the vessel. Forces generated by Eq. (1) reflected not only the depth change but also the local curvature of the 3D physical shape, which was a very intuitive shape descriptor. This was, again, because Eq. (1) is a product of factors: if the line was curved in the viewing plane, then the rendered force changed direction during exploration, if it was curved in the z direction, the magnitude of the force changed. Thus, all three components of curvature were experienced.

This scheme would break down at places where the space curve tangent was orthogonal to the screen. To deal with this problem, Eq. (1) was regularized to become:

$$\vec{F} = -k \frac{dz}{dl} \frac{\vec{\eta}}{1 + \lambda \frac{dz}{dl}} \quad (2)$$

where λ is a small constant compared to one. It simply associated a vanishing local tangent projection to the strongest acceptable force.

3.6 Subjects

Eight students from McGill University were paid for participating in the experiment. They all completed the required trials. The subject pool consisted four males and four females. Subjects’ age ranged from 20 to 53. Seven of them were right handed, one was left handed. Subjects were asked to use their dominant hand. None of them reported any disability related to the use of their hand. All had some experience with a computer mouse, but none had experience with a haptic device. They had wide diversity of educational backgrounds,

which consisted of mining metallurgy, social science, English literature, law, music, mechanical engineering, chemical engineering, bio-informatics and micro-electronics. Except for one subject who had a bio-informatics background, they had no knowledge of the anatomy of the cerebral vessels. They were not informed of the purpose of the experiment prior testing and had no knowledge of the nature of the stimuli prior to the training period.

3.7 Procedure

Subjects were asked to practice for a number of trials without any preliminary screening test. The haptic device was placed at the side of the user and close to the computer screen. Subjects were asked to sit on a chair approximately 60 cm away from the computer screen, with their dominant hand holding the stylus as if they were writing. The other hand was placed on the computer keyboard. Subjects were instructed to push the stylus downward to experience the sliding forces, and to simultaneously watch the cursor on the screen. Subjects then had to explore back and forth the curve segment between the red and green dots and had to make a decision on which was closer to her. When the subject felt that a decision could be made, she would press on key marked with the corresponding color. When the decision was acknowledged, the computer would automatically prompt the subject to proceed with next trial. If after a few tens of seconds, a subject was still unable to make a decision, she would give her best guess and proceeded to the next trial. During the training period, the force feedback gain was adjusted for maximum subjective comfort.

During the training periods, all subjects were provided with the correct answer once they gave their own. To avoid possible recall of the shape, the practice trials were done with artificial data: a straight line and a line undulating in a plane, instead of the actual vessel network. There were no other differences between the training trials and the experimental trials. The feedback provided was intended to help a subject build up the relationships between the stimuli and the shapes. A training period was judged to be completed when a subject could navigate and control the cursor effortlessly while experiencing the sliding forces when desired. They also had to be comfortable

with building the correspondence between shape and a force pattern. The general duration of a training period was between 5 to 20 minutes, depending on how comfortable the subjects were with 3D concepts.

The subjects were then informed that their decisions and the time they spent on making them would automatically be recorded and the actual trials would begin. They were then encouraged to proceed quickly and accurately. They were also informed of the importance of accuracy over speed.

There were 9 different viewing conditions with 40 degree difference in viewing azimuth angle. Viewed under these conditions, the network produced 102 monotonic depth-changing segments, one for each experimental trial.

4 Results

One hundred and two trials for each of the eight subjects produced 816 trials. There were 18 trials with a decision making time smaller than 0.1 seconds and 11 trials with a time larger than 60 seconds. These 29 trials with either too short or too long decision making time were considered as outliers and were discarded, leaving 787 trials for the following analysis.

4.1 Terminology

- *A trial segment or a segment:* A general 3D curved piece of vessel centerline bounded by red and green marks.
- *Segment length:* The number l of voxels contained in a segment (size of one voxel: 0.5 mm).
- *Depth difference:* The depth difference δz in the viewing direction between the two ends of a segment. δz depended on the viewing direction.
- *Mean depth difference:* The ratio between the depth difference δz and the length of a segment, i.e., $\delta z/l$.
- *Mean curvature:* The ratio of the half sum of absolute curvatures at each point of a segment and of its length, c_{mean} .
- *Max curvature:* The maximum of the absolute local curvature along a segment. It reflected the degree of maximum bending of a segment, c_{max} .
- *Measure of segment complexity:* Factors such as depth difference, mean depth difference, mean curvature and maximum curvature of a segment were used to measure the complexity of a segment.

A quantity with an overline refers to the group mean of a quantity. For example, $\overline{\delta z}$ represents the average of depth difference of a specific group, it is the average over many trials and is different from $\delta z/l$, the mean depth difference over a single segment.

4.2 Task Accuracy

There were 765 trials yielding a correct answer and 22 trials yielding an incorrect one. The mean accuracy was calculated as the ratio of the number of trials with a correct response over the number of all trials. It was equal to 97.2%, with a standard deviation of $\sigma_{\text{accuracy}}=16.5\%$. The range of true mean accuracy based on the mean of the sampled subject pool was [95.7% – 98.7%] at 99% confidence interval. If the outliers were not removed, the mean accuracy would have been 96.1% and the standard deviation would have been $\sigma_{\text{accuracy}}=19.4\%$.

The trials were classified into two groups according to the task accuracy. A statistical analysis was carried out to understand whether such factors as decision making time and complexity of segments were related to task accuracy. Group I consisted all of the trials associated with the incorrect answers and Group C contained the trials with correct answers.

The average decision making time was $\overline{t_I}=18.29$ s and $\overline{t_C}=13.55$ s, where the indices refer to the Group I and C, respectively. The variances of t_I and t_C were statistically equal with $F(21,764)=1.07$, $p > 0.10$. This equality of variances justified the results of the following two-sample t test. $\overline{t_I}$ and $\overline{t_C}$ were significantly different, $t(785)=2.23$, $p < 0.02$. $\overline{t_I}$ outlengthed $\overline{t_C}$ by [0.56, 8.92] seconds at a 95% confidence interval. That is, on average, the trials associated with incorrect answers took a longer decision making time than the trials with correct answers. The two-sample t test revealed that there were no significant difference between $\overline{\delta z_I}$ and $\overline{\delta z_C}$, $t(785)=1.19$, $p > 0.2$.

Similarly, there was no significant difference between $(\overline{\delta z_I/l_I})$ and $(\overline{\delta z_C/l_C})$, $t(785)=0.51$, $p > 0.5$; no significant difference between $\overline{c_{I-\text{mean}}}$ and $\overline{c_{C-\text{mean}}}$, $t(785)=0.082$, $p > 0.5$; and no significant difference between $\overline{c_{I-\text{max}}}$ and $\overline{c_{C-\text{max}}}$, $t(785)=0.76$, $p > 0.4$. In other words, no significant difference due to the complexity of segments was found to be associated with the accuracy of the

answer. A subject was able to make statistically the same accurate depth discrimination, regardless of the complexity of a segment. More specifically, there was no observed direct relationship between the magnitude of depth difference and discrimination accuracy.

To analyze the relationship between the accuracy of depth discrimination and length of a segment, the trials were grouped according to the length of segments into three groups: short segments group, medium length segments group and long segments group. The mean accuracy for each of the groups were 97.0%, 96.8% and 97.8% respectively. Based on this, it could be concluded that no effects of the length of segments on depth discrimination accuracy was observed.

4.3 Decision Making Time

The histogram in Fig. 7a indicates that the decision making time was skewed with a long tail. To induce normality in order to meet the normal distribution requirement for analysis of variance (ANOVA), a logarithmic transformation was applied. A Lilliefors test confirmed that the logarithmically transformed decision making time was a normal distribution (see Fig. 7b).

The average of decision making time, \bar{t} of the sampled pool was 13.68 s, with standard deviation $\sigma_t=9.87$ sec. If the outliers were not discarded, then \bar{t} and σ_t would be 14.2 and 12.3, respectively. The range of true value of decision making time, based on the sample mean of the tested subjects, was [12.77, 14.59] seconds at 99% confidence interval.

The trials were classified into two groups again, but according to the decision making time instead of the task accuracy used in the previous section. A statistical analysis was again done to understand whether or not the complexity of a segment had some effects on the length of decision making time.

Group L consisted all of the trials whose decision making time were longer than the average and Group S contained the rest of the trials. There were 283 and 504 trials in groups L and S, respectively, with $\overline{t_L}=23.8$ and $\overline{t_S}=8.00$ seconds and $\overline{\delta z_L}= 2.193$ and $\overline{\delta z_S}= 2.322$. Group L had a larger depth difference over the segments than that of Group S, $t'(558.7)=1.6$, $p \simeq 0.1$, which is marginally significant. Here, the Welch test was

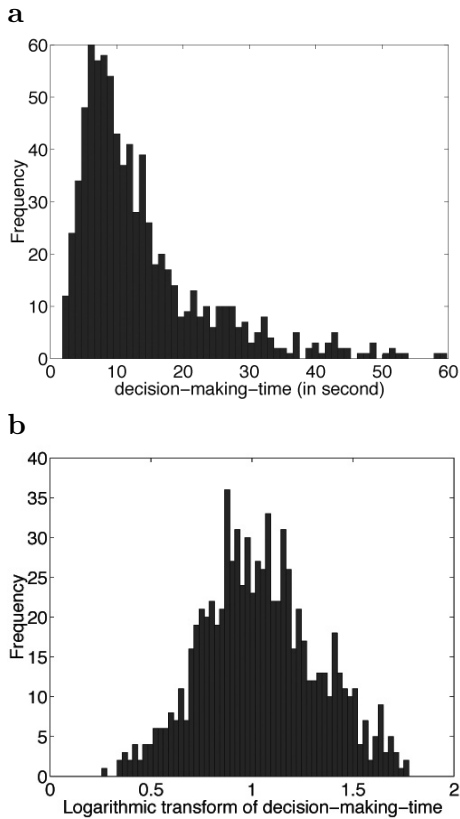


Fig. 7. **a.** Frequency histogram of decision-making-time. **b.** In logarithmic coordinates.

used instead of the two-sample t test as the equality of the variances was not justified [1]). Similarly, $(\overline{\delta z_L/l_L})=0.0461$ and $(\overline{\delta z_S/l_S})=0.0504$ which meant that Group S had a larger depth gradient along the segments, and this difference was statistically significant, $t'(575.5) = 3.496$, $p < 0.001$. $\overline{c_{L-\text{mean}}}=0.052$ and $\overline{c_{S-\text{mean}}}=0.047$, so Group S had a smaller mean absolute curvature than that of group L and this difference was again statistically significant, $t'(439.4) = 2.96$, $p < 0.005$; $\overline{c_{L-\text{max}}}=0.211$ and $\overline{c_{S-\text{mean}}}=0.1674$. Group S had less absolute maximum curvature than that of Group L, and again this difference was statistically significant, $t'(401.8)=2.27$, $p < 0.05$. In other words, complex segments in terms of smaller depth difference and larger curvature caused a subject to use a longer time to discriminate the relative depth of its ends. There was no observed effects of the length of segments on the task completion time. The mean task completion time for short, median and long segments group were 12.86, 14.25 and 14.12 seconds, respectively.

4.4 Inter-Subjects Variance

This section is intended to analyze the inter-subjects variance in accuracy and decision making time. Statistically all subjects performed equally well in terms of task accuracy, $F(7,779)=2.08$, $p > 0.01$. However, at $p < 0.05$ level, the subjects' performance varied. This was doubly confirmed by a χ^2 test with $\chi^2(7) = 14.4325$, $0.01 < p < 0.05$. The decision making time was significantly different among different subjects, $F(7,95)=20.68$, $p < 0.01$. Table I lists the performance of each of the subjects.

Subject	1	2	3	4	5	6	7	8
Mean (s)	14.3	12.0	16.9	12.8	12.3	14.9	18.5	7.8
Acc'y (%)	94.1	100	94.0	98.0	95.0	98.0	99.0	99.0

TABLE I

SUBJECTS' MEAN DECISION TIME AND ACCURACY.

Subjects with some experience with 3D concepts, either from their educational background (one subject was a mechanical engineer) or from working experience (one subject in music once did a 3D perception project in arts) performed better than others. Mean decision time for male and female were 13.11 and 14.24 seconds, respectively, $t(785) = 1.61$, $p > 0.05$. Mean accuracy for male and female were 98.21% and 96.22%, $t(785) = 1.694$, $p > 0.05$. Male subjects' performance was not statistically different from that of female subjects, in terms of task completion time and accuracy.

4.5 Control Experiment

The above results clearly indicated that the integrated display system can be used to effectively inform a user of the depth relationships between two points on a segment within around a dozen of seconds. However, it remained unclear whether the observed performance was entirely due to force feedback. One control experiment was performed to resolve this question. Here, all the conditions were the same as that of the previous one, except that the intensity of the force feedback was zero. Three subjects participated, and all of them had already participated the main experiment five to ten days before. Subjects were instructed and trained to visually inspect the intensity gradient change of the visual cue and its orientation to discriminate

the depth relationship. The other conditions of the experiment were the same as that of the previous one. The average of task accuracy was 54% with standard deviation 50% and decision making time was 11.95 seconds with standard deviation $\sigma=9.5$.

	With	Without
Mean Accuracy (%)	97.2%	54%
Mean decision time (s)	13.68	11.95

TABLE II

MEAN ACCURACY AND DECISION TIME WITH AND WITHOUT FORCE FEEDBACK ACROSS ALL SUBJECTS.

The ANOVA revealed significant effects of force feedback on the accuracy, $F(1, 786) = 1277$, $p < 0.01$ and on the decision making time $F(1, 786) = 217$, $p < 0.01$. With force feedback, the task was completed with higher accuracy and longer time than in conditions without force feedback. The results on performance with both force feedback on and off are summarized in Table II.

5 Summary and Conclusion

The experiment and the control showed that subjects could deal effectively with depth during static viewing of angiograms. It is possible that other display schemes could be more time efficient, however the proposed method is particularly parsimonious in terms of the hardware and software resources it requires. This suggest that an integrated static-visual/2D-haptic visualization system can effectively be used to estimate the depth relationships between regions of a complicated, naturally occurring data set, within around a dozen of seconds, and that force feedback was effective when used with our three-factor force rendering scheme. Hence it is possible to envisage using force feedback to free up vision for other tasks such as symbolic information display.

A further finding is that performance accuracy is not significantly related to the complexity of a shape, at least in the range we have tested. A viewer can discriminate depth relationships equally well regardless of the details of the shape of a segment.

Task performance time, however, increases with more complex shapes. A complex shape, especially the one with sharp turns (in our case, a segment

with high curvature) requires finer motor control, and hence more time, to explore it. For segments with smaller depth difference, the depth-gradient is smaller and thus it takes longer for a subject to discriminate the depth relationship between its two ends. This observation suggests that force intensity is related to the haptic information bandwidth. Higher force intensity may corresponds to higher bandwidth. However, this needs further research to be confirmed.

The subjects did not report any fatigue after completing both the training and the experimental trails, although they lasted from 30 to 60 minutes. No statistically significant difference observed between the performance of males and females. Subjects have often reported visual fatigue after completing the reference trials when the force feedback was turned off. This is because the visual stimulus associated to the interaction point was small (9×9 pixels) and required much attention to discriminate its changes since it was the only source of information in that case.

Additional operation modes could be designed along the lines of the scheme described in this paper. For example, in a context of augmented reality, “rubber bands” could be entrained between arbitrary locations in a 3D space and their depth relationship experienced haptically. While the present study was limited to the perception of relative depth within vessels segments of angiograms, the same scheme could be adapted to convey the relative depth of, say, a vessel and the site of a pathology. The quantity dz could refer to the change of distance of virtual 3D lines drawn between sites of interest but that are viewed only in 2D. This would be helpful during the planning and verification phases of minimally invasive neurological procedures done from a fixed view point, for example, restricted by accessibility constraints. In such cases, it is inevitable that the vessel segments representation occupies the same screen region as where the pathology is shown. The haptic cue proposed in this paper is one of the very few that could be used to quantitatively resolve the depth dimension.

In this study, we dealt with lines, but extensions to surfaces were explored using a similar force rendering scheme and a 2D haptic device [6]. If we consider data with one or more dimensions (such

as opacity) embedded in 3D space, then a 3D device would be required but for lines and surfaces, 2D haptics appears to be usable. For higher dimensional or 3D nonscalar data sets, it would be possible to use a two DOF force display device, provided its inputs had richer possibilities than moving in a plane. Future work could consider comparing what exactly is gained by moving from 2D to 3D haptics and should explore the perceptual aspects related to this question.

Many issues are still unresolved, for example, related to the design of optimal work areas, to the effect of mappings between the haptic stimuli and the visual stimuli, to clarify more precisely the effect of fatigue, and so-on. In the meantime this study confirms that haptic feedback can provide useful improvements to current visualization platforms given very little added complexity and cost.

6 Acknowledgements

The angiographic data set used was kindly provided by Dr. Hua Qian from the Robert Research Institute (RRI) in London, Ontario, Canada.

This research was supported by IRIS-III, the Institute for Robotics and Intelligent Systems. Additional funding was provided in the form of a McGill Wong Fellowship to the first author, and by NSERC, the Natural Sciences and Engineering Council of Canada, in the form of an Discovery Grant for the second author.

References

- [1] Affi, A. A. and Azen, S. P. 1972. *Statistical Analysis: A Computer Oriented Approach*, Academic Press.
- [2] Avila, R. S. and Sobierajski, L. M. 1996. A Haptic Interaction Method for Volume Visualization, *IEEE Proceedings of Visualization 96'*, pp. 197–204,
- [3] Charland, P. and Peters, T., 1996. Optimal display conditions for quantitative analysis of stereoscopic cerebral angiograms. *IEEE Transactions on Medical Imaging*, Vol. 15, No. 5, pp. 648–656.
- [4] Ehrlicke, H. H., Donner, K., Koller, W., and Straber, W. 1994. Visualization of Vasculature From Volume Data, *Computer Graphics*, Vol. 18, No. 3, pp. 395–406.
- [5] Pfister, H., Hardenbergh, J., Knittel, J., Lauer, H. and Seiler, L. 1999. The Volume-Pro Real-Time Ray-Casting System. Proc. *ACM SIGGRAPH'99*, pp. 251–260.
- [6] Hayward, V., Yi, D. 2003. Change of Height: An Approach to the Haptic Display of Shape and Texture Without Surface Normal. In *Experimental Robotics VIII*, Springer Tracts in Advanced Robotics, Siciliano, B. and Dario, P., (Eds.), Springer Verlag, New York. pp. 570–579.
- [7] Heidrich, W., McCool, M., and Stevens, J. 1995. Interactive Maximum Projection Volume Rendering. Proc. *IEEE Visualization'95*, pp. 11–18.
- [8] Hong, K. C. and Freeny, P. C. 1999. Pancreaticoduodenal Arcades and Dorsal Pancreatic Artery: Comparison of CT Angiography with Three-Dimensional Volume Rendering, Maximum Intensity Projection, and Shaded-Surface Display. *American journal of roentgenology (AJR)*, Vol. 172, pp. 925–931.
- [9] Hurmuzlu, Y., Ephanov, A., and Stolanovici, D. 1998. Effect of a Pneumatically Driven Haptic Interface on the Perceptual Capabilities of Human Operators. *Presence: Teleoperators and Virtual Environments*, Vol. 1, No. 3, pp. 290–307.
- [10] Infed, F., Brown, S. V., Lee, C. D., Lawrence, D. A., Dougherty, A. M., and Pao, L. Y. 1999. Combined Visual/Haptic Rendering Modes for Scientific Visualization, Proc. *8th Annual Symposium on Haptic Interfaces for Virtual Environment and Teleoperator Systems*.
- [11] Iwata, H. and Noma, H. 1993. Volume Haptization, Proc. *IEEE 1993 Symposium on Research Frontiers in Virtual Reality*, pp. 16–23.
- [12] Kuszyk, B. S., Heath, D. G., and Ney, D. R. 1995. CT Angiography with Volume Rendering: image findings. *American journal of roentgenology (AJR)*, Vol. 165, pp. 445–448.
- [13] Mroz, L., Hauser, H., and Groller, E. 2000. Interactive High quality maximum intensity projection. *Computer Graphics Forum*, 19(3).
- [14] Ney, D. R., Fishman, E. K., Magid, D., and Drebin, R. A. 1990. Volumetric rendering of computed tomography data: principles and techniques. *IEEE Computer Graphics and Applications*, Vol. 2, No. 2., pp. 24–32.
- [15] Pao, L. Y. and Lawrence, D. A., 1998. Synergistic VisualHaptic Computer Interfaces, *Proceeding JapanUSA Vietnam Workshop on Research and Education in Systems, Computation and Control Engineering*, Hanoi, Vietnam, pp. 155–162.
- [16] Shi, Y. and Pai, D.K., 1997. Haptic Display of Visual Images, *IEEE Annual Virtual Reality International Symposium*, pp. 188–191.
- [17] Sollenberger, R. L. and Milgram, P. 1993. Effects of Stereoscopic and Rotational Displays in a Three-Dimensional Path-Tracing Task. *Human Factors*, Vol. 35, No. 3, pp. 483–499.
- [18] Wang, Q. 1999. *Translation of Graphic to Haptic Boundary Representation*, M.Eng. Thesis. McGill University, Electrical Engineering Dept.
- [19] Yi, D. and Hayward, V. 2002. Skeletonization of Volumetric Angiograms for Display, *Computer Methods in Biomechanics and Biomedical Engineering*, Vol. 5, No. 5, pp. 329–341.